# Spatiotemporal variability of winter wheat phenology with response to weather variability

ATIKUL HOQUE (S2534827)

Enschede, The Netherlands

Internship report submitted to the Deutsche Zentrum für Luft- und Raumfahrt (DLR) and the Faculty of Geo-Information Science and Earth Observation of the University of Twente in partial fulfilment of the requirements for the Internship course (201900002) of Master of Science in Geo-information Science and Earth Observation.

Specialization: Natural Resource Management

EXTERNAL SUPERVISOR:
Martina Wenzl

INTERNAL SUPERVISOR:
Dr. Michael Schlund

**Acknowledgements**

Foremost, I would like to express my sincere gratitude and thanks to my supervisor Martina Wenzl for providing me with this wonderful opportunity to carry out my internship at DLR and for her guidance, encouragement, and support throughout the period. I would also like to express my gratitude to Dr. Michael Schlund to guide me as an internal supervisor during my internship and for his valuable suggestions. I am grateful to Belinda Jaarsma – Knol for her guidance and management of the formal procedures during the beginning of the internship. I would like to further extend my gratitude towards the Erasmus+ mobility fund for providing me with the housing and travelling allowance in Bavaria, Germany. I would also like to acknowledge my friend Nitheshnirmal Sadhasivam who was my housemate during my stay in Bavaria. We both shared our meals together, had informative chats and travelled around the beautiful landscapes of the Bayern region, which helped me keep motivated and focused. I would also like to thank my house owner Conny Von Roehl for providing me with a friendly and cozy place to stay during the period. And last but not least, I would like to acknowledge DLR for having me as an intern.

# Table of Contents

# List of Figures



# List of Tables

**Overview of the report:**

The overall work is conducted throughout the internship at DLR. The internship assignment can be categorized into two broad categories. The initial part contains pre-processing of Invekos dataset using QGIS and Python, which will be used later for crop type classification using machine learning for the entire Germany. The latter part involves the analysis of spatial and temporal variability of winter wheat across Mecklenburg-Vorpommern, which will be considered as the main part of this report.

**Part one: Pre-processing of the parcel (Invekos) data**

The pre-processing of the Invekos parcel data consists of several steps which are summarized in **Figure 1**.

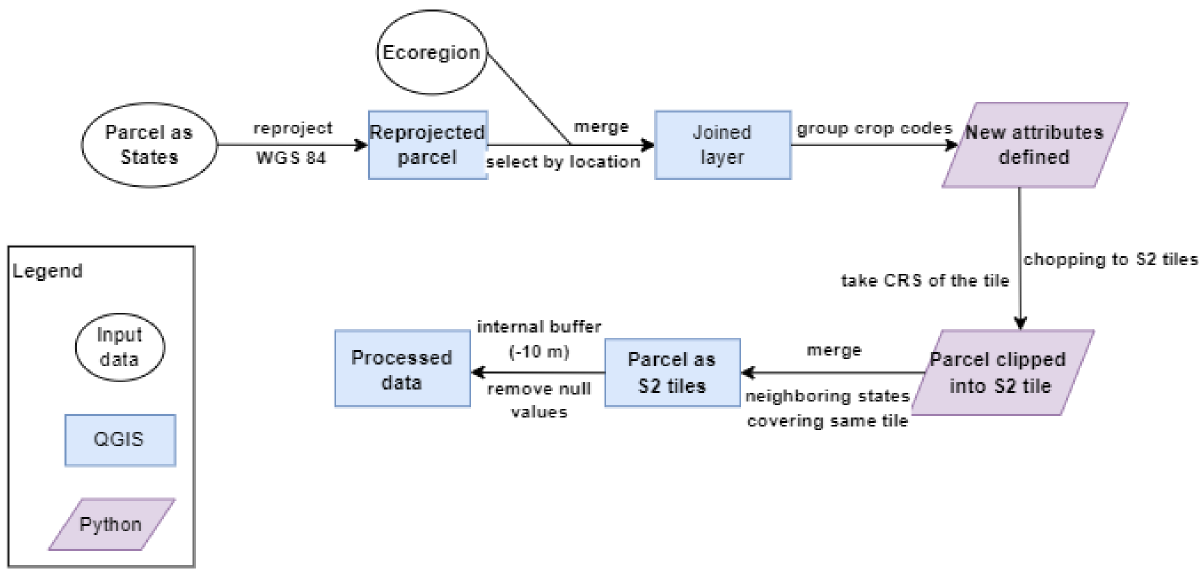


**Figure 1** Steps followed to pre-process the invekos dataset for crop type map classification

**Part two: Winter wheat phenology**

## 1. Introduction

Vegetation phenology refers to the recurring patterns of vegetation development and their linkages to the climate (White et al., 1997). Different phenological phases and their properties, such as rate of green-up, amplitude and rate of vegetation growth, occurrence and rate of senescence, are key indicators of ecosystem dynamics and help us understand the global environmental changes (Xiao et al., 2009). For crops, the partition of biomass to different organs is controlled by phenology which is strongly related to the optimal timing of different management decisions (Wang et al., 2015). Furthermore, it helps in monitoring and modelling yields, helping in better management practices for aiming toward better food quality (Schwartz, 2013).

Previous studies demonstrate that variability of weather/climate impacts the development and production of field crops (Misra, 2013). Crop phenology is primarily influenced by temperature and photoperiod for a given cultivar, but it can also be controlled by water, nutrients level, and management practices. Increased mean temperature around the globe has resulted in a shorter growing season meaning less absorbed radiation, which leads to less biomass and yield (Siebert & Ewert, 2012). Winter wheat is highly susceptible to temperature change, and recent temperature increases led to advance sowing dates in western Germany (Rezaei et al., 2018).

Crop phenology has been extensively studied using different data-driven crop models (Challinor et al., 2009; Jamieson et al., 2007). On the other hand, direct phenological trend analysis based on field observation data received far less attention. Hence, this study will focus on the analysis of field in-situ phenology data from German Meteorological Service (Deutscher Wetterdienst – DWD) to find out the timing, trend and variability of winter wheat in Mecklenburg-Vorpommern, a northern state in Germany. Furthermore, the study will incorporate Sentinel-2 (S2) remote sensing data to evaluate and complement the findings and trends from the in-situ data. Temporally frequent remote sensing data offer a unique capability to look into temporal profiles of crops ranging from local to global scales (Zeng et al., 2020). Vegetation Indices (VIs e.g., NDVI, EVI) from S2 are good data sources to monitor vegetation trends because of their higher spatial and temporal resolutions. Finally, temperature and weather data will be integrated to explain the spatial and temporal variability of phenophases. Therefore, the objectives of this study are:

a) To extract relevant time periods for winter wheat fields from the phenology raster dataset for 2018 to 2021.
b) To calculate vegetation Indices (NDVI and EVI) from S2 data for those time periods and compare the development with phenophase developments.
c) To retrieve temporal profiles from EVI and match them with the phenophase developments.
d) To find variability of VIs and phenophases across different ecoregions, soil types, and different years.
e) To integrate weather data and compare phenological development with it across different years.

# 2. Study Area and Dataset

## 2.1 Study Area

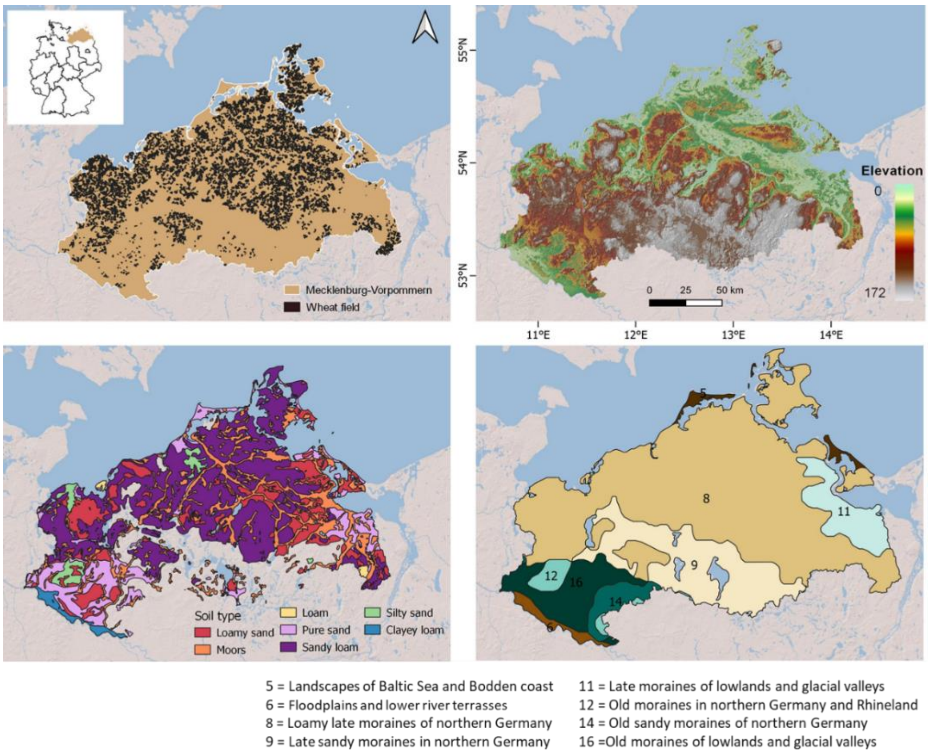


**Figure 2** Overview of the study area with winter wheat fields of 2021, elevation, soil type and ecoregion

German northern federal state of Meckelnburg-Vorpommern is selected as the study area. An overview of the study area is presented in **Figure 2**. The advantage of this region is winter wheat is widely cultivated across the state, and a wide range of in-situ phenology observations is available (DWD, 2021). On average, 13000 fields are cultivated as winter wheat annually for the studied years with a mean area of 30 ha. The fields are more concentrated on the northern side of the state and the elevation ranges up to 172 m in the state. There are seven different soil types in the study area, with sandy loam being the dominant type. Among the eight ecoregions in the state, loamy late moraine consists the majority of the site.

## 2.2 Dataset

In-situ phenology data:

Ground phenology observations were retrieved as raster file from DWD. It contains a large database of crop phenological observations for a long period. Volunteer surveyors gather the field information and report two or three times per week. The observations take place over the same field which is located within a distance of 5 km from the phenology stations (Kaspar et al., 2015). The dataset comes as point data from the station, which is later converted into raster using a method called 'phenological forecasts'. The raster conversion includes statistical components which combines reported statistics of the crops and regional distribution of observation dates. A detailed summary of the method is available in Janssen (2020).The used phenological stages for this study for wheat are shown in **Table 1**.

| Phenophases | BBCH scale | Field photos |
|---|---|---|
| Cultivation | 0 | |
| Leaf development | 10 |  |
| Stem elongation | 31 |  |
| Heading | 51 |  |
| Milk ripeness | 75 |  |
| Ripening | 87 |  |
| Harvest | 99 | |

**Table 1** Studied phenophases along with their sample field photos (Larsen et al., 2008)

Sentinel-2:

Sentinel-2 data were retrieved using Google Earth Engine platform. Surface Reflectance products (Level-2A) were used from the collection "COPERNICUS/S2_SR" for the period of interests. To remove clouds, cloud shadows and snow contaminated pixels, a simple algorithm was adopted following Housman et al. (2018). Hence, the non-contaminated pixels are retained for extracting vegetation indices.

Reference data:

Field parcel data were extracted from the Integrated Administration and Control System (IACS) which manages the payment of agricultural subsidies to the farmers. It provides parcel level spatial information about agricultural land use annually. The information is reported by farmers hence it is not free from errors. Wheat fields *(Winterweizen)* is taken from the dataset for the periods of interests. An internal buffer of 10 m is taken from each side of every parcel and removed in order to avoid the edge effect of the field boundaries. Finally, parcels which are smaller than one hectare are removed.

Weather data:

Gridded monthly precipitation data were obtained from DWD Climate Data Center (CDC, ftp://ftp-cdc.dwd.de). Data for the months corresponding to phenological dates were only used to find out if there is any correlation between weather and phenology.

Soil and Ecoregion:

Ecoregions are delineated based on similar characteristics in terms of topography, climate, hydrography, soil and geology. Each ecoregions are coded from one to 86 by DWD. The soil dataset consists of seven broad soil categories.

# 3. Method

## 3.1 Calculation of Vegetation Indices

Enhanced Vegetation Index (EVI) and Normalized Difference Vegetation Index (NDVI) were calculated for the relevant time periods (phenophase stages) based on the pre-processed S2 data in Google Earth Engine (Gorelick et al., 2017) using the following equations.

$$\text{NDVI} = \left(\frac{NIR - RED}{NIR + RED}\right) \quad (1)$$

$$\text{EVI} = G\left(\frac{NIR - RED}{NIR + (C1 * RED - C2 * BLUE) + L}\right) \quad (2)$$

where NIR, RED, and BLUE are reflectance in Near Infrared, Red, and Blue regions. G is determined by the C value which is calculated by linear fitting (RED = c * NIR). C1 and C2 are coefficients to correct aerosol scattering, and L is a soil adjustment factor. In most studies, the following values are used for these parameters: G = 2.5, C1 = 6.0, and L = 1 (Huete et al., 1999). Mean values of EVI and NDVI are taken for all the parcels of respective years. Furthermore, mean EVI and NDVI values per soil class and per different ecoregions are also taken to see if there is any spatial variations. Finally, values are visualized in bar plots for respective years.

### 3.2 Extracting Temporal profiles

Temporal profiles using the mean EVI and NDVI values of the pre-processed S2 data are generated for all the field parcels for the defined years. Locally weighted scatterplot smoothing (LOESS) is used to smooth the time series. The smoothing can reduce the impact of extreme values or outliers. Finally the smoothed temporal profile will be used to compare it's correspondence with the field phenophases.

### 3.3 Link with weather data

Mean value is taken from the three month (April, May, and June) temperature and precipitation data and maps are generated to show the spatial and temporal variability of both the weather phenomena. Finally, two scatter plots are generated showing temperature and precipitation values against the mean phenophases to define the relationship between the two variables.

## 4. Results and discussions

### 4.1 Time periods across the phenophases

Time periods of different phases across the studied years are extracted from the phenology raster data and plotted in **Figure 3**. It is evident that there are temporal variations across different stages for different years. In almost all the stages, phases came earlier in 2018 and for 2021, phases came later than the others. Ripening shows the most variations in terms of temporal variability. For instance, the mean day of year for ripening in 2018 was 187 (6 July), whereas for 2021 it was 197 (16 July).

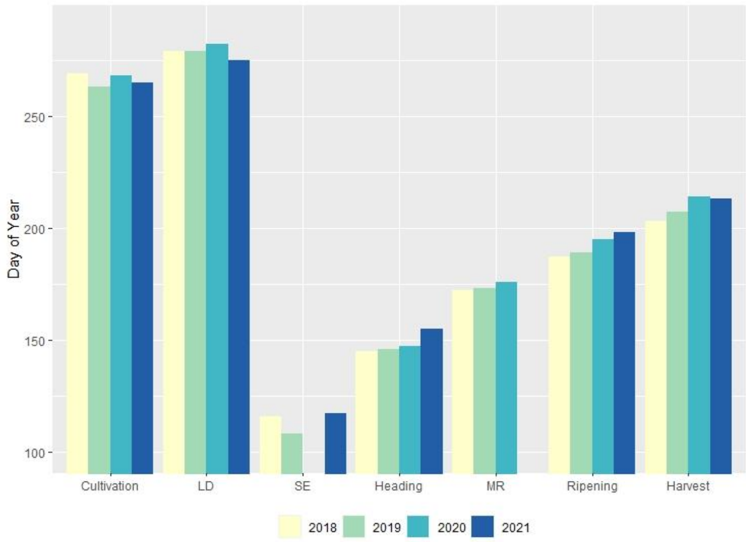


**Figure 3** Median values of Day of Year (DOY) of different phenophases across four studied years

### 4.2 Temporal variations of phenophases

**Figure 4** shows the temporal variations of the phenophases in terms of EVI and NDVI values among the studied years. In general, both the indices shows a similar pattern. However, NDVI values tend to be a bit lower than that of EVI values which can be explained with the saturation effect of high biomass and soil conditions on NDVI (Matsushita et al., 2007). Hence, for the rest of the analysis, only EVI values are shown.

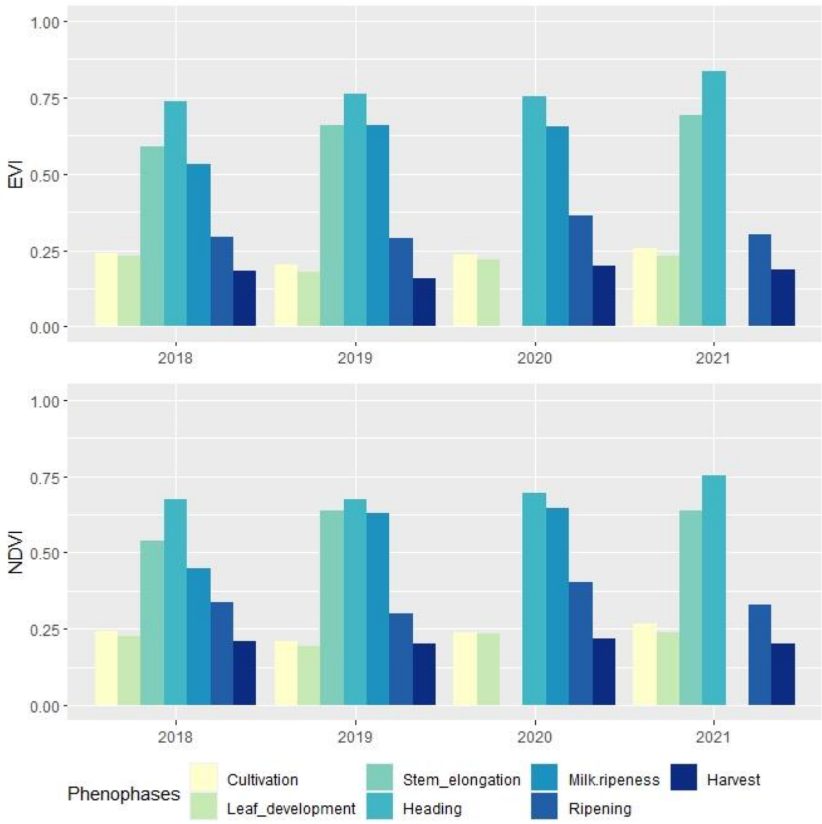


**Figure 4** EVI and NDVI values of phenophases to show the temporal variations across different years for the phenophases

It is evident that the indices values are lower for 2018 for stem elongation, heading, milk ripeness and ripening stages than the rest of the years. These are the important growing stages of a wheat's life cycle where optimum weather condition plays a crucial part in the crops development (Peñuelas et al., 2002).

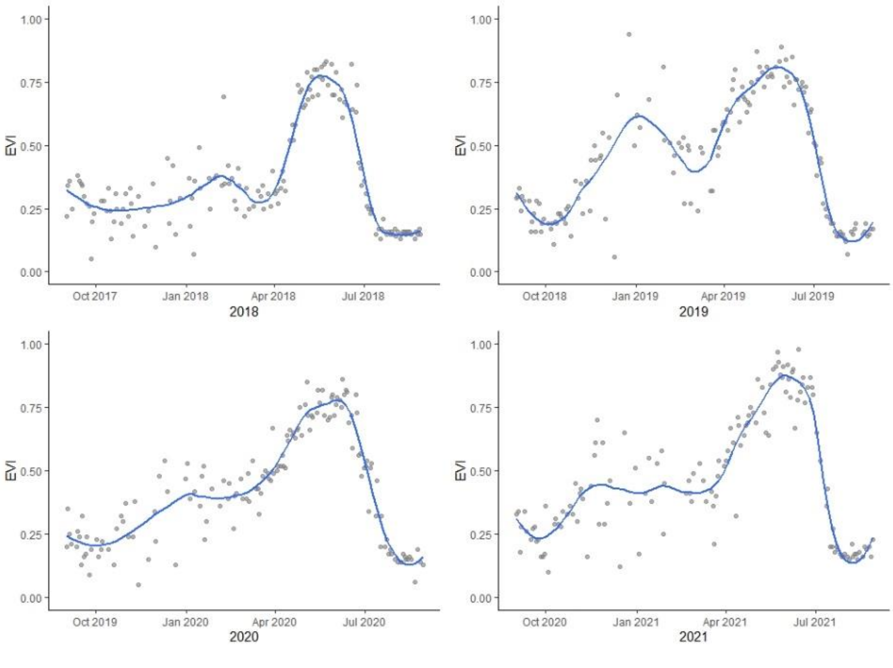


**Figure 5** EVI temporal profiles from the mean values of all the winter wheat parcel for different years. Dots represent the EVI values of the respective dates and the line is the LOESS smoothing to show the trend

For 2018, a significant decrease of values is noted in Stem elongation and milk ripeness. 2019 and 2020 maintains more or less similar patterns among themselves across all phases, while for 2021, values are a bit higher. The variations in indices values reflect the variations of DOY of phenophases. Hence, remote sensing indices are well aligned with the field phenophase values which is also found by previous studies (Mercier et al., 2020; Zhang et al., 2003). From the temporal profiles of different years from **Figure 5**, it can be concluded that the season of 2018 was shorter than the other three seasons resulting in early harvest dates. Previous studies also concludes that increasing temperature resulted in shorter phenological phases leading to early harvests (Estrella et al., 2007).

## 4.3 Variations of phenophases by soil type

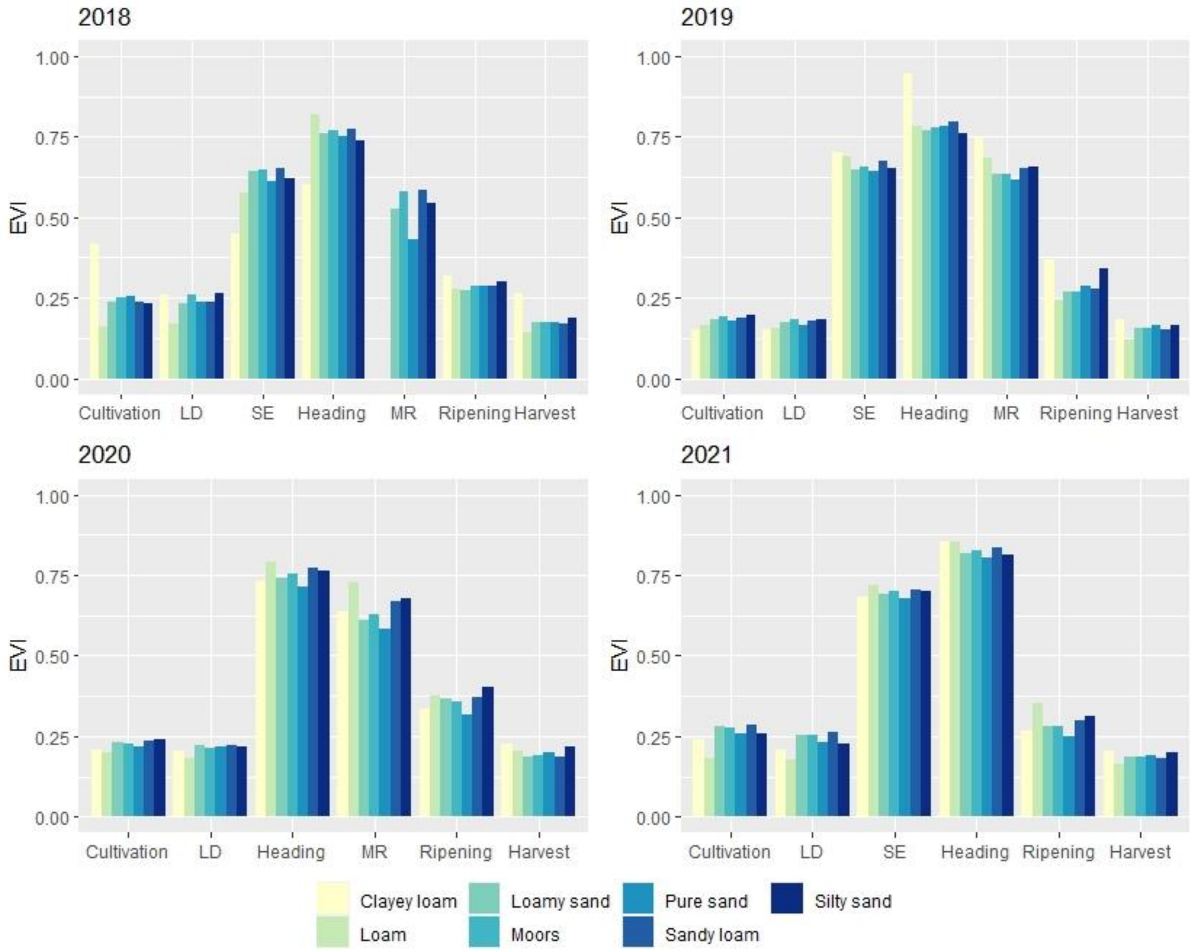


**Figure 6** EVI values across different soil types for the phenophases

Overall, both the clayey loam and loamy soils shows higher EVI values than other soil types (**Figure 6**). On the other hand, pure sand has the lowest overall values across different phases and years. The reason might be due to poor water retention rate in sandy soils which acts as a driver for lower plant productivity (Wong & Asseng, 2006). The other soil types maintains more or less similar values. However, it can be noted that, the used soil type dataset is coarse in resolution with broad classes. Hence, a more detailed soil map might produce more accurate results.

## 4.4 Variations of phenophases by ecoregion

More variability is evident across different ecoregions than soil types. Phases generally come earlier in the 'Floodplains and lower river terraces' as well as 'Late moraines of lowlands and glacial valleys' ecoregions whereas it comes late in the 'Loamy late moraines' and 'Late sandy moraines' ecoregions (**Figure 7**).

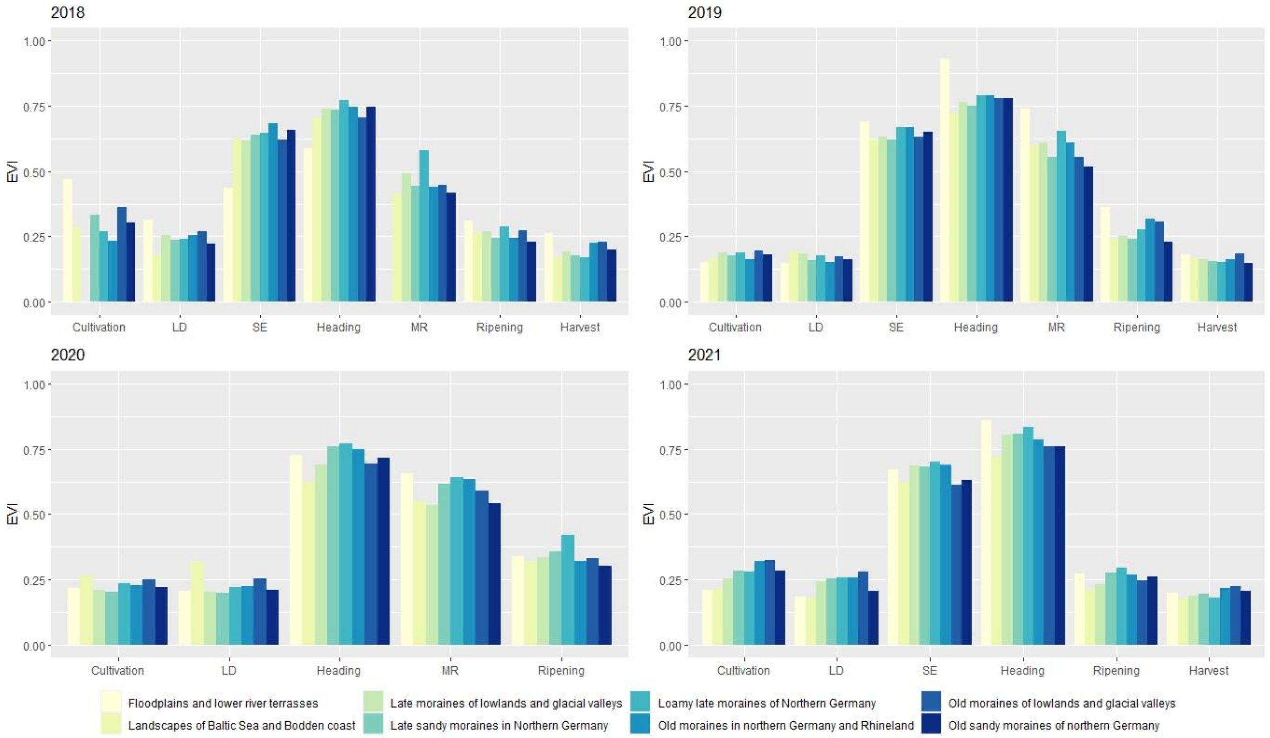


**Figure 7** EVI values for different ecoregions for the phenophases

As there are more variations across the heading stage for ecoregions, day of year for different ecoregions are shown for that stage in **Figure 8**.

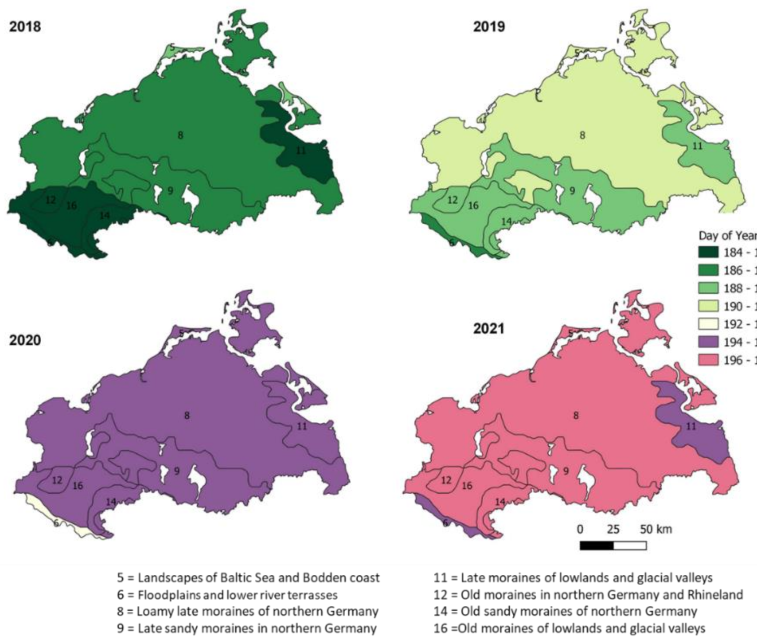


**Figure 8** DOY of phenophases across different ecoregions to show the spatial and temporal variability of winter wheat

It is apparent from the map that ecoregions in the southern part experienced the phase earlier than their northern counterpart. A similar north-south gradient of phenophases was noted by (Siebert & Ewert, 2012)

## 4.5 Integration of weather data

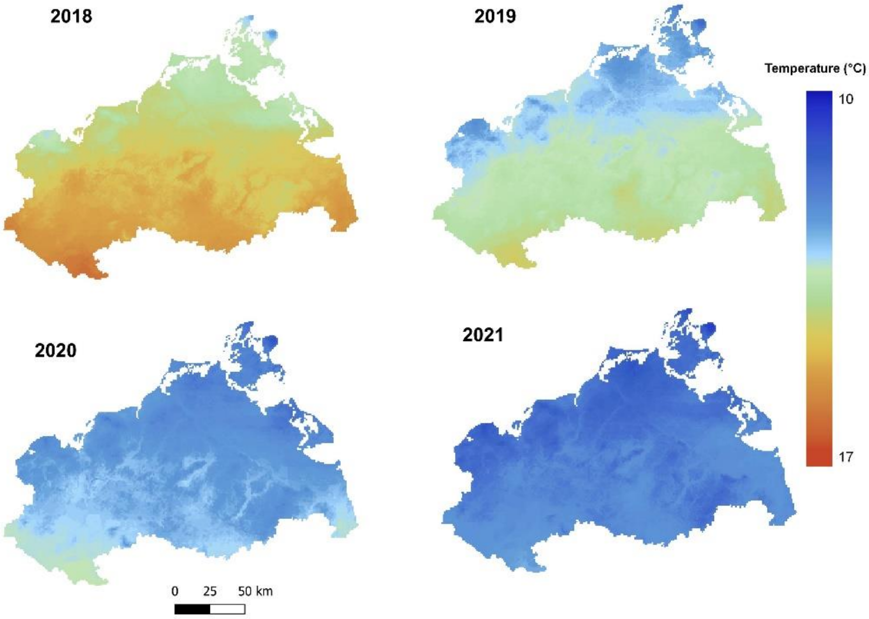


**Figure 9** Mean monthly temperature of April, May and June

**Figure 9** shows that 2018 was the warmest of all the years whereas 2021 was the coldest. There is also north to south spatial variation in recorded temperature for all the years. The northern part experienced colder days than their southern counterpart. The low mean temperature in the northern coastal areas can be explained by cooling effect of sea temperature (Siebert & Ewert, 2012).

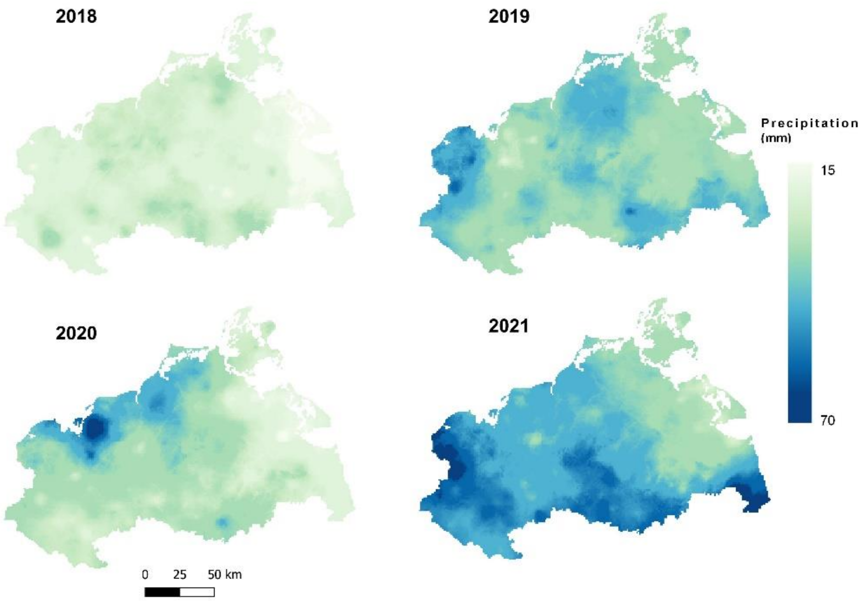


**Figure 10** Mean monthly precipitation of April, May and June

A similar pattern is evident in recorded precipitation dataset plotted in **Figure 10**. 2018 was driest of all the years, however there is no clear spatial variation across north to south. On the other hand, 2021 was the wettest year where in the southern and western part it received most of its precipitation.

## 4.6 Relationship between phenophases and weather

**Figure 11** shows a clear pattern about the relationship between temperature and occurrence of the phenophases.

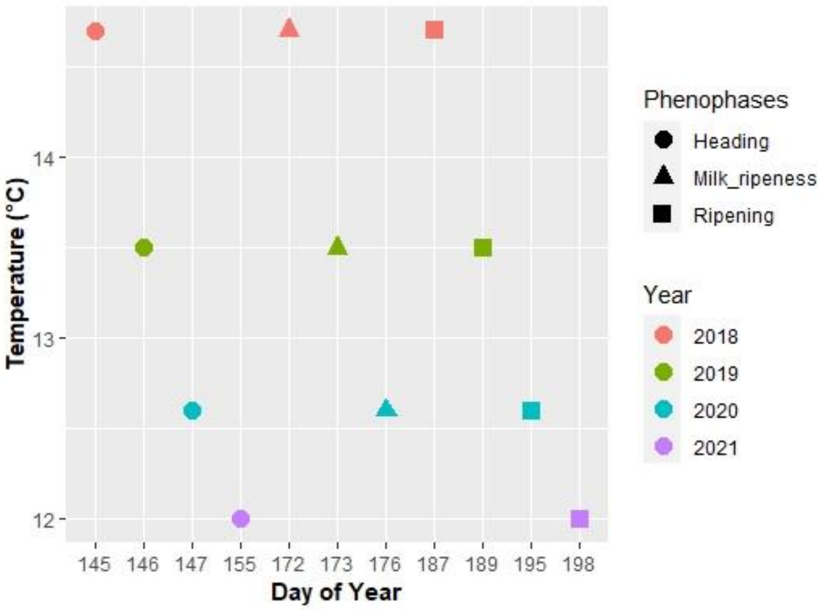


**Figure 11** Scatterplot showing temperature values in y-axis and day of year values on the x-axis for three major phenophases (heading, milk ripeness, and ripening) for the studied years

For example, 2018 was the warmest of all the years and the phases came earlier than other three years. On the other hand, 2021 was the coldest of the four years and the phases came later than others. This positive relationship between temperature and phases were reported by earlier studies (Chmielewski et al., 2004; Estrella et al., 2007; Siebert & Ewert, 2012). However, to clearly define the relationship between phenophases, only visual observation might not be enough. Therefore, logistic regression might be necessary to come to a plausible conclusion, which can be way forward for future research. Furthermore, as there are other factor involved such as management practices, it is hard to classify that weather is solely responsible for the phenology variations.

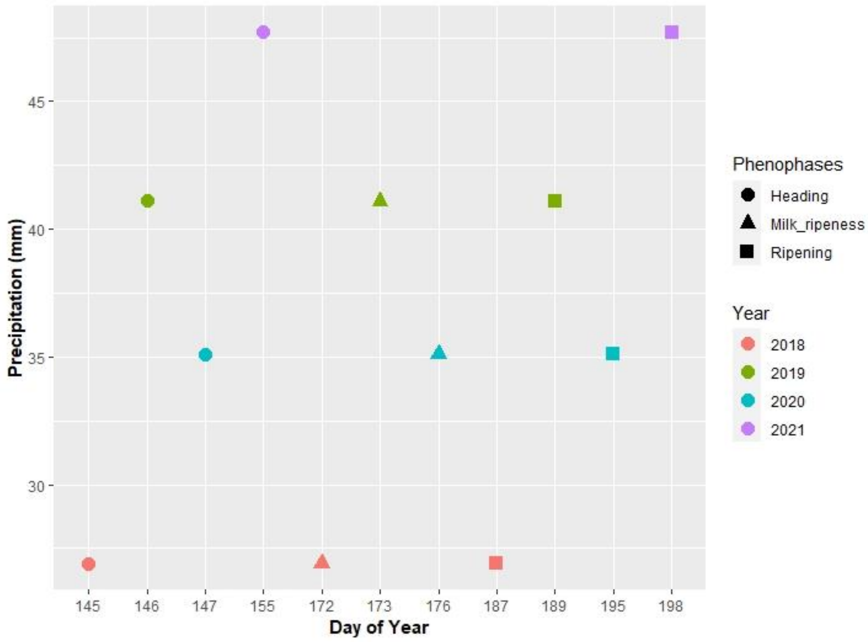


**Figure 12** Scatterplot showing precipitation values in y-axis and day of year values on the x-axis for three major phenophases (heading, milk ripeness, and ripening) for the studied years

There is no clear pattern seen from **Figure 12** between precipitation and phenophases.

# 5. Conclusion and outlook

## 5.1 Conclusion

Overall the spatial and temporal variations of the phenophases as well as of the EVI values are evident. Both the temporal profiles imitate the in-situ phenophases very well. Variability across different soil type and ecoregion is also evident from the study. Finally, because of extreme weather condition in 2018, almost all the phases came earlier than usual. Farmers had to harvest the crop earlier than expected as well. On the other hand, 2021 was the coldest year among the four studied years, and the phases came a bit later.

## 5.2 Limitations

1) Monthly weather data is coarse to define relationship between different phases and weather phenomena.
2) Only four data points might be too little to conclude about the relationship.
3) Due to time constrains, it was not possible to calculate remote sensing based phenometrics from the temporal profiles.
4) No statistical significance test was used

## 5.3 Recommendations for future studies

1) Remote sensing based phenometrics can be retrieved and compared with in-situ phenophases for the wheat fields.
2) Using daily weather data to relate the phenology with weather phenomena
3) Integrating length of the day can also be an interesting input to see if it has any relationship with phenophases.

## 6. References


Challinor, A. J., Ewert, F., Arnold, S., Simelton, E., & Fraser, E. (2009). Crops and climate change: progress, trends, and challenges in simulating impacts and informing adaptation. *Journal of Experimental Botany*, *60*(10), 2775–2789. https://doi.org/10.1093/JXB/ERP062

Chmielewski, F. M., Müller, A., & Bruns, E. (2004). Climate changes and trends in phenology of fruit trees and field crops in Germany, 1961–2000. *Agricultural and Forest Meteorology*, *121*(1–2), 69–78. https://doi.org/10.1016/S0168-1923(03)00161-8

DWD. (2021). *Wetter und Klima - Deutscher Wetterdienst - Berlin und Brandenburg*. https://www.dwd.de/EN/weather/weather_climate_local/berlin-brandenburg/bbb_node.html

Estrella, N., Sparks, T. H., & Menzel, A. (2007). Trends and temperature response in the phenology of crops in Germany. *Global Change Biology*, *13*(8), 1737–1747. https://doi.org/10.1111/J.1365-2486.2007.01374.X

Gorelick, N., Hancher, M., Dixon, M., Ilyushchenko, S., Thau, D., & Moore, R. (2017). Google Earth Engine: Planetary-scale geospatial analysis for everyone. *Remote Sensing of Environment*, *202*, 18–27. https://doi.org/10.1016/J.RSE.2017.06.031

Housman, I. W., Chastain, R. A., & Finco, M. v. (2018). An Evaluation of Forest Health Insect and Disease Survey Data and Satellite-Based Remote Sensing Forest Change Detection Methods: Case Studies in the United States. *Remote Sensing 2018, Vol. 10, Page 1184*, *10*(8), 1184. https://doi.org/10.3390/RS10081184

Huete, A. R., Didan, K., Huete, A., Didan, K., Leeuwen, W. van, Jacobson, A., Solanos, R., & Laing, T. (1999). *MODIS VEGETATION INDEX (MOD 13) ALGORITHM THEORETICAL BASIS DOCUMENT Principal Investigators Development Team MODIS Product ID: MOD13*. http://vip.arizona.edu

Jamieson, P. D., Brooking, I. R., Semenov, M. A., McMaster, G. S., White, J. W., & Porter, J. R. (2007). Reconciling alternative models of phenological development in winter wheat. *Field Crops Research*, *103*(1), 36–41. https://doi.org/10.1016/J.FCR.2007.04.009

Janssen, W. (2020). *Phänologie-Journal Erstellung phänologischer Prognosen*. *54*, 54. https://www.dwd.de/DE/fachnutzer/freizeitgaertn

Kaspar, F., Zimmermann, K., & Polte-Rudolf, C. (2015). An overview of the phenological observation network and the phenological database of Germany's national meteorological service (Deutscher Wetterdienst). *Advances in Science and Research*, *11*(1), 93–99. https://doi.org/10.5194/ASR-11-93-2014

Larsen, R. J., Smith, P., Cowbrough, M., Falk, D. E., Quesnel, G., & Baute, T. (2008). *A field guide to cereal staging. | Directory of scientists and professionals*. https://profils-profiles.science.gc.ca/en/publication/field-guide-cereal-staging

Matsushita, B., Yang, W., Chen, J., Onda, Y., & Qiu, G. (2007). Sensitivity of the Enhanced Vegetation Index (EVI) and Normalized Difference Vegetation Index (NDVI) to Topographic Effects: A Case Study in High-density Cypress Forest. *Sensors 2007, Vol. 7, Pages 2636-2651*, *7*(11), 2636–2651. https://doi.org/10.3390/S7112636

Mercier, A., Betbeder, J., Baudry, J., le Roux, V., Spicher, F., Lacoux, J., Roger, D., & Hubert-Moy, L. (2020). Evaluation of Sentinel-1 & 2 time series for predicting wheat and rapeseed phenological stages. *ISPRS Journal of Photogrammetry and Remote Sensing*, *163*, 231–256. https://doi.org/10.1016/J.ISPRSJPRS.2020.03.009

Misra, A. K. (2013). Climate change impact, mitigation and adaptation strategies for agricultural and water resources, in Ganga Plain (India). *Mitigation and Adaptation Strategies for Global Change*, *18*(5), 673–689. https://doi.org/10.1007/S11027-012-9381-7/TABLES/7

Peñuelas, J., Filella, I., & Comas, P. (2002). Changed plant and animal life cycles from 1952 to 2000 in the Mediterranean region. *Global Change Biology*, *8*(6), 531–544. https://doi.org/10.1046/J.1365-2486.2002.00489.X

Rezaei, E. E., Siebert, S., Hüging, H., & Ewert, F. (2018). Climate change effect on wheat phenology depends on cultivar change. *Scientific Reports 2018 8:1*, *8*(1), 1–10. https://doi.org/10.1038/s41598-018-23101-2

Schwartz, M. D. (2013). Phenology: An integrative environmental science. *Phenology: An Integrative Environmental Science*, 1–610. https://doi.org/10.1007/978-94-007-6925-0

Siebert, S., & Ewert, F. (2012). Spatio-temporal patterns of phenological development in Germany in relation to temperature and day length. *Agricultural and Forest Meteorology*, *152*(1), 44–57. https://doi.org/10.1016/J.AGRFORMET.2011.08.007

Wang, N., Wang, J., Wang, E., Yu, Q., Shi, Y., & He, D. (2015). Increased uncertainty in simulated maize phenology with more frequent supra-optimal temperature under climate warming. *European Journal of Agronomy*, *71*, 19–33. https://doi.org/10.1016/J.EJA.2015.08.005

White, M. A., Thornton, P. E., & Running, S. W. (1997). A continental phenology model for monitoring vegetation responses to interannual climatic variability. *Global Biogeochemical Cycles*, *11*(2), 217–234. https://doi.org/10.1029/97GB00330

Wong, M. T. F., & Asseng, S. (2006). Determining the Causes of Spatial and Temporal Variability of Wheat Yields at Sub-field Scale Using a New Method of Upscaling a Crop Model. *Plant and Soil 2006 283:1*, *283*(1), 203–215. https://doi.org/10.1007/S11104-006-0012-5

Xiao, X., Zhang, J., Yan, H., Wu, W., & Biradar, C. (2009). Land surface phenology convergence of satellite and CO2 eddy flux observations. *Phenology of Ecosystem Processes: Applications in Global Change Research*, 247–270. https://doi.org/10.1007/978-1-4419-0026-5_11/FIGURES/6_11

Zeng, L., Wardlow, B. D., Xiang, D., Hu, S., & Li, D. (2020). A review of vegetation phenological metrics extraction using time-series, multispectral satellite data. *Remote Sensing of Environment*, *237*, 111511. https://doi.org/10.1016/J.RSE.2019.111511

Zhang, X., Friedl, M. A., Schaaf, C. B., Strahler, A. H., Hodges, J. C. F., Gao, F., Reed, B. C., & Huete, A. (2003). Monitoring vegetation phenology using MODIS. *Remote Sensing of Environment*, *84*(3), 471–475. https://doi.org/10.1016/S0034-4257(02)00135-9